CONTROL AND SIMULATION OF HYBRID POWER GENERATION SYSTEM OPERATING IN GRID CONNECTED AND STAND ALONE MODE

Ridha BENADLI[1,2] **Brahim KHIARI**[1]
[1]LANSER Laboratory, *CRTEn, B.P.95 Hammam-Lif 2050, Tunis-Tunisia*
[2]National Higher Engineering School of Tunis, EED, BP 56, Montfleury 1008, Tunis, Tunisia
Anis SELLAMI
[2]National Higher Engineering School of Tunis, EED, BP 56, Montfleury 1008, Tunis, Tunisia

Abstract: *This paper presents the modelling, analysis, performance and the synthesis of control of Hybrid Renewable Energy System (HRES), with Battery Energy Storage System (BESS). This HRES can also be connected to the grid and capable to be, with a storage device, a stand-alone operation. The Photovoltaic (PV) generator is controlled via DC-DC boost converter by using Incremental Conductance (InCond) method to search optimum operating point of this source. The BESS is used to maintain the DC bus voltage at a constant value by charging or discharging this storage using a bidirectional DC-DC converter. The wind generator is controlled via AC-DC converter with an MPPT method that allows optimal transfer of wind power for a wide range of wind speeds. The control for the wind generator is based on an indirect vector control by the Filed Orientation Control (FOC) where one makes it possible to perfectly follow the optimum characteristic of the wind turbine. In a Stand-Alone Mode (SAM) operation, the Voltage Source Converter (VSC) is used for the controlled output voltage in terms of amplitude and frequency delivered to the AC load. In Grid Connected Mode (GCM) operation, the VSC is used to control the electrical grandeurs on the grid. Performed validations by simulation in Matlab/Simulink have clearly demonstrated the effectiveness and performance of the control strategies developed for the control of power converters.*

Key words: *Control, Grid-connected, Stand-alone, Hybrid Renewable Energy System, Wind turbine, Photovoltaic; Battery energy storage system.*

1. Introduction

A hybrid system interconnected by a set of renewable energy sources and storage systems help to ensure greater energy availability and optimize maximum power generation systems, both from technical and economic point of view. This type of system is widely used in low power applications; isolated sites or connected to the grid. The common DC bus interconnected various sources of production and storage system is used before converting this energy into alternating current. Among renewable energy sources, we chose wind and PV. The combination of these two sources can help to achieve a more continuous electricity production. This study is directed to PV/ wind systems connected to the grid and able to work in SAM through the BESS. This storage is used as a backup source to power the system when the renewable energy source is unavailable. Other backup sources can be used for the production of renewable sources of hollow periods with or without BESS such as fuel cells [4, 8, and 18], supercapacitors, the energy storage flywheel [19], diesel generators [14]. Conversely, when the energy produced is greater than the energy consumed, the excess electricity is stored in the BESS [5], supercapacitors [13] and with an electrolyzer hydrogen tank [4]. However, fuel cells are very expensive and the diesel generator operate at a mediocre performance with high power consumption grows with their request. This energy management is difficult to achieve but it may be necessary in applications in isolated site to ensure the balance between the power consumed by the user and the power produced by the sources.

Several studies have investigated the hybrid production system. This study concerns the modeling, analysis and synthesis of control and management strategies of the hybrid system. In [15], a management algorithm in a PV/ wind hybrid system with BESS powering a housing loads in parallel with the grid is described. In [2, 3] authors shows the modeling, the analysis and the control of energy from a PV /wind power system with BESS powering the AC load in parallel with the grid. [18], provides the control of a PV/ wind system/ fuel cell for supplying only DC load. In reference [5], authors proposed a control of a PV/wind system operating in both SAM and GCM, but this system is valid only for a single phase. In reference [1], authors presented a control of PV/ wind power, but this system needs an energy storage system to ensure continuity of supply local loads AC islanding mode. Also, in reference [10], the authors are silent about the use of an energy storage device of a hybrid system to supplying AC loads in parallel to the grid.

Different strategies proposed for the control of the bidirectional buck-boost converter to ensure a balance of

power through charging /discharging of the battery. Reference [6] presents the control and quality of wind power with battery pack. The Reference [7], develops the control and management of a PV /battery system connected to the grid. In references [6, 17], a control strategy by a single control loop of the voltage with the Proportional Integral (PI) is proposed. Reference [10] proposes a control strategy with two regulation loop; a voltage loop with the PI and a current control by hysteresis and a voltage regulation loop. Similarly in Reference [4, 9], but the current control with the PI. This strategy is used in our study to the control of the bidirectional converter. It ensures dynamic meshing performance higher than other technology cited above through the internal loop current.

Several standalone converter control strategies have been proposed to set the amplitude and frequency delivered to AC loads off grid. In references [16, 17], a control strategy with six PI controllers in a photovoltaic/wind power the fuel cell proposed. Another strategy to control with a single PI controller in a PV/ battery /supercapacitors was proposed in [13]. In [6, 9] propose a control strategy by two control loop (current / voltage) with four PI controllers in a wind hybrid system. This latter strategy is used in our study to the control of the bidirectional converter in operation out electric grid.

Different strategies proposed in the literature to control the three-phase PWM voltage converter in a renewable energy based production system connected to the electrical grid [1, 4, 19]. All these strategies aim to achieve the same objectives, namely: a power factor near the unit, sinusoidal current is absorbed in phase with the voltage. The most popular is the technique known as the Voltage Oriented Control (VOC) [15]. This technique is used in our study to control the electrical grandeur of the grid becauce ensures high dynamic and static performance through third by the loop current internal regulations.

The developed HRES as shown in Fig.1 constitutes of wind subsystem 10 kW equipped of a direct driven permanent-magnet synchronous generator (PMSG), a PV array 7.625 kW, a BESS, a DC bus (650V), power interfaces and a set of control system. This figure also shows the power balance of the renewable energy conversion system in the two modes operation of HRES.
. This paper is organized as follows: In Section 2, proposed architecture of grid-connected with wind and PV resources. The modeling components of the proposed hybrid system in Section 3. The control strategies of hybrid system in Section 4. Simulation results and discussion are given in Sections 5. Conclusion is addressed in the last section.

2. Proposed hybrid system architecture

Fig. 1 shows the overall architecture of the proposed grid-connected hybrid system with wind and PV resources. The two energy sources are connected in parallel to a common dc bus line through their individual dc-dc converters. Combining multiple renewable resources via a common dc bus of a power converter has been prevalent because of convenience in integrated monitoring and control and consistency in the structure of controllers as compared with a common ac type [12]. The wind subsystem involves a turbine is a small power wind equipped with a PMSG, a diode rectifier and a boost converter for the tracking of the maximum power point using a perturbation and observation (P&O) method, a three-phase inverter. The solar subsystem consists of a PV array controlled by another boost converter used for the maximum power point tracking (MPPT). The PLL is used to detect the phase angle of the grid voltage for the control. The simple inductors L are used as a filter interfacing inverter and mains. The LCL filter provides advantages in costs and dynamics since smaller inductors can be used. However, in a grid-connected system, an LCL filter may cause resonance, which is a disaster for the system's stability [5]. For the inverter, an integral sliding mode controller has been used for the current controller because can eliminate the steady-state error by adding integral sliding surface. The SMC presents attractive features such as robustness to parametric uncertainties of the wind turbine and the generator as well as to electrical grid disturbances [13]. The current-controlled SVPWM inverter is adapting to three-phase PV/WT grid-connected system.

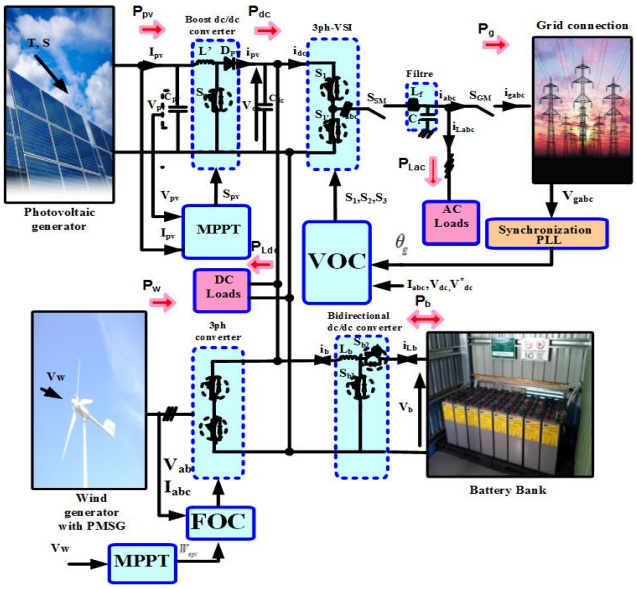

Fig.1. Control Structure of a PV-Wind hybrid system

2. Modeling the different components of the hybrid system.

2.1. PV array model

There are two types of photovoltaic PV modules: electrical model with a diode or two diodes. Among which we chose to model a diode because it is the simplest to implement and most used in the literature. This model is composed of a parallel current generator with a diode in parallel and two resistors (R_s series / shunt R_{sh}) as illustrated

in Fig.2. The two resistors R_s and R_{sh} represent respectively the various contact resistances and connections and leakage currents.

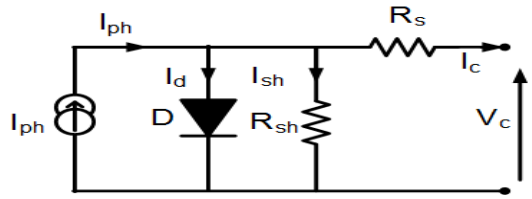

Fig. 2. Electrical model equivalent of a PV cell

The current generated by the PV array is given by [17]

$$I_{pv} = N_p I_{ph} - N_p I_s \left\{ \exp\left[q\left(\frac{V_{pv} + R_s I_{pv}\left(N_s / N_p\right)}{N_s nKT} \right) - 1 \right] \right\} - N_p \frac{\left(V_{pv} + R_s I_{pv}\left(N_s / N_p\right)\right)}{R_{sh} Ns} \quad (1)$$

Where I_{ph} is the photocurrent, I_s is the reverse saturation current of the diode, n is the ideality factor of the diode, q is the electron charge (q = 1.6.10^{-19}), k is the Boltzmann's constant (k = 1.38.10^{-23}), and T is the solar array panel temperature.

In order to get the desired electrical power which is 7,625 kW peak power, we placed 5 modules connected in series (N_s=5) and 5 modules connected in parallel (N_p=5).

The output power and current of PV array delivered by the PV array in function of voltage for different irradiance levels is shown in Fig.3, this allows us to easily observe the influence of solar irradiation on the Maximum Power Point (MPP) and short circuit current (I_{sc}).

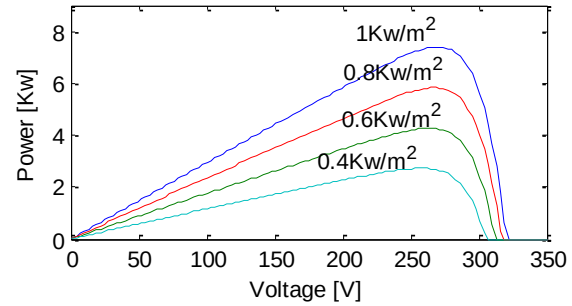

Fig. 3. P-V and I–V output characteristics of the PV array

2.1. Wind turbine model

The mechanical power captured by the blades of a wind turbine is given by [12]

$$P_w = \frac{1}{2}\rho C_p\left(\lambda,\beta\right)\pi R^2 v_w^3 \quad (2)$$

Where, ρ is the air density (kg/m^3), R is the rotor radius of wind turbine,v_ω is the wind speed in m/s, C_p is the turbine rotor power coefficient, which is a function of tips speed ratio λ and pitch angle β.

$$\lambda = \frac{R w_m}{v_w} \quad (3)$$

Where w_m is the rotor speed of the wind turbine.

The maximum power generated by the wind turbine is given by

$$P_w = k_{opt} {w_m}^2 \quad (4)$$

Where, $k_{opt} = \frac{1}{2}\rho.A.C_{p_{opt}}\left(\frac{R}{\lambda_{opt}}\right)^2$ (5)

The justification for Eq.(4) as shown in Fig.4, on which it is noted that for each value of the wind speed was a maximum power point correspond to different speeds of rotation of the turbine. The idea for adapting the power extracted in the rotational speed of the turbine.

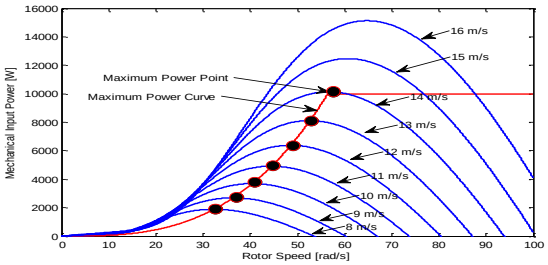

Fig. 4. Output power generated by a turbine for different wind speeds

2.3. Battery storage model

In order to guarantee the availability of energy in the DC and AC loads even in unfavorable weather conditions and in both mode of the bidirectional converter, we use the battery as energy storage dispostif. The modeling of this battery is implemented in Ref [16, 17]. It can be illustrated by the equivalent circuit as shown in a Fig.5. This model consists of a source votage E_0 in series with a resistor R_b, where the voltage source is described by

$$E = E_0 - K\frac{Q}{Q - \int i\,dt} + A\exp\left(-B\int i\,dt\right) \quad (6)$$

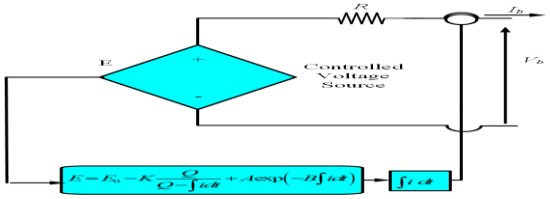

Fig. 5. Lead-acid battery model.

2. Control of power converters

3.1 Photovoltaic MPPT control

The control of the DC/DC boost converter allows both elevateing the value of the PV array to obtain the desired DC bus voltage and searching for the MPP. The principle of any MPPT methods is to act on the duty cyclic of the converter to ensure that the generator is operating at its maximum value no matter how the climatic conditions will be. In our study, we chose the InCond method [2,3]. The principle of this method is based on the conductance G and calculates its incremental ΔG, if the conductance $G > \Delta G$, the operating point is left of MPP, it is right if $G < \Delta G$. The flow chart of this method is illustrated in the Fig. 6.

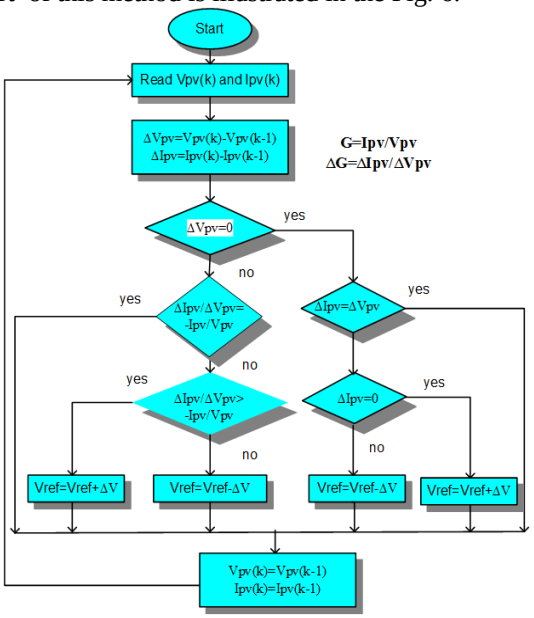

Fig. 6. Flow chart of InCond method

3.1 control of bidirectional buck-boost converter

Fig. 7 shows the block diagram of the proposed control of bidirectional buck-boost DC-DC converter using PI controller. This converter works in boost mode when the switch S_1 is ON (discharging the battery) and buck mode when the switch S_2 is ON (charging the battery).

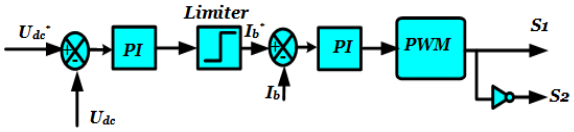

Fig. 7. Control of bidirectional buck-boost converter

3.3 Generator side control

The control of generator side converter enables the search of maximum power point in such a manner to minimize the error between the operating power and maximum power. The Fig.8 shows the principle of control installed for the wind source. The three-phase voltages generated by PMSG will be adjusted of space vector modulation (SVM) vector modulation receiving the reference voltages of control at speed imposed by the maximum extraction power MPPT device.

The reference speed imposed by MPPT is given by

$$w_{m-opt} = \frac{\lambda_{opt} V_w}{R} \quad (7)$$

Where λ_{opt} is the maximum torque coefficient.

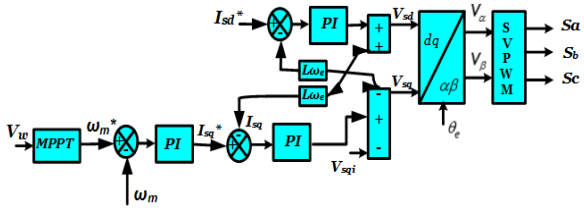

Fig. 8. Control of generator side converter

3.1 Grid side control

The hybrid production system can also be connected to the grid and capable, with a storage device, a standalone operation. In an SAM, the VSC is used in a voltage control mode control strategy for regulating autonomously the amplitude and frequency of the AC loads. Fig. 9 shows the block diagram of the VSI control strategy in *d-q* coordinates described in [9]. The line voltage and frequency are set to 230 V rms and 50 Hz respectively.

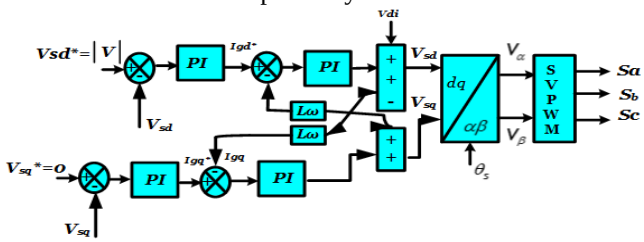

Fig. 9. Control for stand-alone mode

In a GCM, we chose a control structure based on two cascaded control loops, an external voltage loop and an inner loop current in a synchronous *d-q* frame. Fig. 10 shows the block diagram of proposed control strategy in this mode. The reference voltages generated at the output of the current regulators (V_α, V_β) and the location information of the grid voltage from Phase locked loop (PLL) block will be sent to a Space Vector Pulse Width Modulation SVPWM.

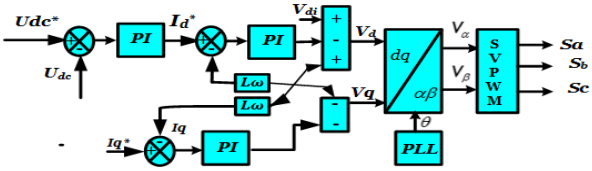

Fig. 10. Control for grid-connected mode

4. Results and discussion

Different simulations results are used to analyze the dynamic performance HRES both GCM and SAM are represented in this work. The overall configuration is shown in Fig. 1 of HRES were simulated by using the Simulink/ Matlab. An option of this system is to connect the sources with the DC, AC load and to the grid via an AC, DC bus. Second option proposed in this study is to connect the sources by only to the DC load via a DC bus.

4.1 Isolated operation with a local DC loads (off grid)

The system is tested for only DC load connected to the DC bus in isolated operation. Fig. 11 illustrate the distribution powers of the HRES with variable input source and load power conditions. Specifically, the wind speed decreases from 12 m/s to 14 m/s at t=1.5s and increases from 12 m/ s to 14 m /s at t=3s, respectively. The solar irradiation varies is increased from 0.8 to 1kW/m^2 at t=1.5 s and decreased from 1kW/m^2 to 0.8 kW/m^2 at t=3s, respectively. The basic power balance equation for the generation sources and the DC load demand is given by

$$P_{pv} + P_w \pm P_b = P_{Ldc} \quad (8)$$

Where P_w is the wind turbine power, P_{pv} is the power generated by the PV array, P_{Ldc} is the DC load demand.

For the first period $t \in [0 \quad 0.8]$, the total generated power from PV and wind is around 12.2kW, the P_{Ldc} is around 8.4kW. The power demand by the load is less than the power produced by the sources. Therefore, the battery is charged with a negative current. For the second period $t \in [0.8 \quad 2]$, the sum of wind and PV generated power is not sufficient to supply the resistive load demand. Under this situation, the battery discharge with a positive current to supply the power loads as shown in Fig. 12.

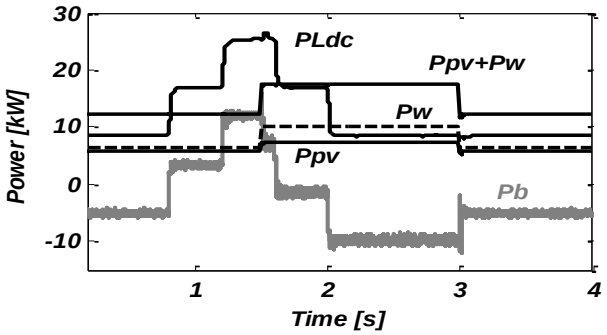

Fig. 11. Various power of the hybrid system (**Case1**)

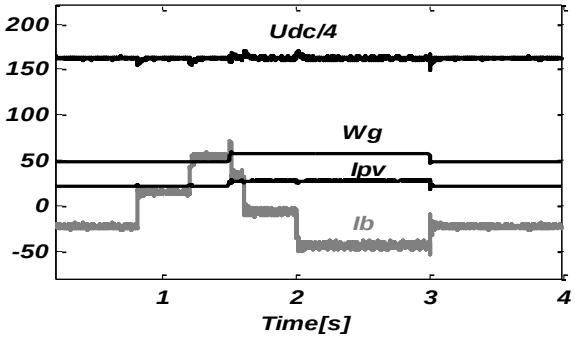

Fig. 12. Hybrid system variables evolution (**Case 1**: U_{dc} is the DC bus voltage [V], W_g is the rotor speed of PMSG [rad/s], I_{pv} is the output current of PV [A], I_b is the battery current [A])

4.2 Isolated operation with a local DC and AC loads (off grid)

The system is simulated in SAM of operation to validate the dynamic performance under varying the load condition, wind speed and in irradiance. Exactly, the irradiance decreases from 1kW/m^2 to 0.7 kW/m^2 at t=1.5s and the wind speed from 14 m/ s to 10 m /s at t=1.5s. The power loads demand P_{Lac} and P_{Ldc} is varied between 15 kW to 19kW and 0 to 4 kW respectively. In this mode, the power difference between the generation sources and the total load demand is calculated as

$$P_{pv} + P_w \pm P_b = P_{Ldc} + P_{Lac} \quad (9)$$

Where P_{Ldc} is the DC load demand.

At period $t \in [0 \quad 0.8]$, the load demand is more than the wind and solar power production. Therefore the required energy is supplied by the battery (positive current and power) as shown in Fig.13 and Fig.14. The VSC is able to regulate the voltage level of local AC load at 230 V and the frequency at 50 Hz as shown in Fig.15.

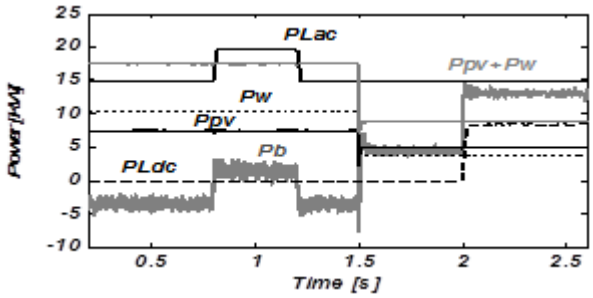

Fig. 13. Various power of the hybrid system (**Case 2**)

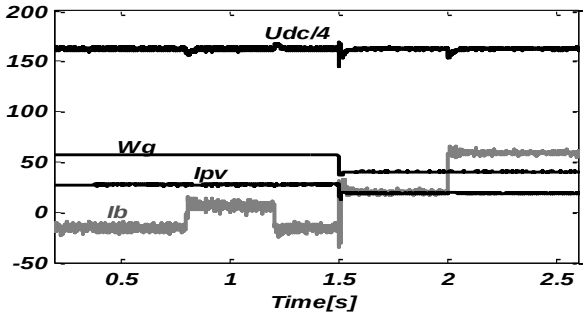

Fig. 14. Hybrid system variables evolution (**Case 2**: U_{dc} is the DC bus voltage [V], W_g is the rotor speed of PMSG [rad/s], I_{pv} is the output current of PV [A], I_b is the battery current [A])

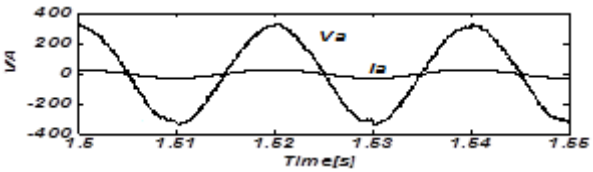

Fig. 15. AC load voltage and current (**Case 2**)

4.3 Grid connected operation

Now consider the system hybrid in GCM. Consider the step change in the DC load power while keeping other variables constant, wile the PV and Wind at their rated power 7.46 kW and 10kW respectively. The AC load demand is fixed at 2kW. In this mode, the exchange power through the grid-side converter and the grid is calculated as

$$P_{inv} = P_{pv} + P_w \pm P_b - P_{Ldc} \quad (10)$$

Where P_{inv} is the real output power from the bidirectional DC-AC converter, the positive value represents means the power flow from the DC bus the AC bus and vice versa.

The exchange power between inverter to the grid can be expressed as

$$P_g = -\left(P_{inv} - P_{Lac}\right) \quad (11)$$

Where P_g *i*s the real power injected into the grid. The negative value represents the injected power to the grid and vice versa.

The power balance equation given in Eq(9) can be written as:

$$P_{net} = P_b = \pm\left(P_{inv} + P_{Lac} - P_{pv} - P_w\right) \quad (12)$$

Fig. 16 shows the control performance of the hybrid system under variable DC load condition. At period $t \in [0 \quad 0.8]$, the sum of power from PV and Wind system (P_{pv}+P_w) is around 17.5 kW, while the value of power DC load demand is set at zero. During this period, the real output power from the bidirectional DC-AC converter is positive (+7 kW). Hence, the DC bus supplies the energy to AC bus. In addition the extra power between P_{inv} and P_{Ldc} is will be injected the grid (P_g=-5 kW). The battery starts charging with a negative limit current as shown in Fig.17. At period $t \in [1.2 \quad 1.8]$, the DC load demand increases to 56 kW, which more than the power net P_{net}. At this moment, the battery turned the discharging mode (positive current I_b).

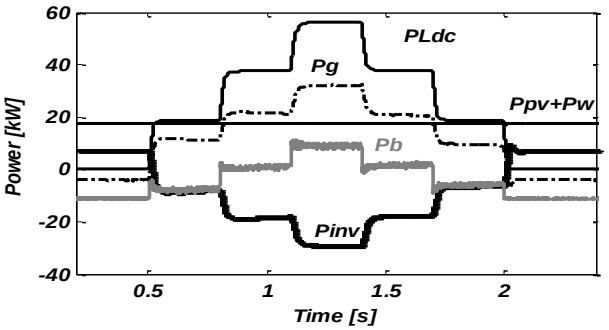

Fig.16. Various power of the hybrid system (**Case 3**)

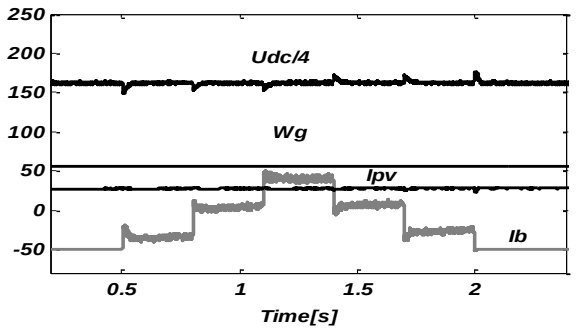

Fig. 17. Hybrid system variables evolution (**Case 3**: U_{dc} is the DC bus voltage [V], W_g is the rotor speed of PMSG [rad/s], I_{pv} is the output current of PV [A], I_b is the battery current [A]).

5. Conclusion

This paper presents a contribution to the analysis of comprtement and mastery of performance of HRES composed of a variable wind speed turbine with PMSG, PV and battery storage system capable of working in stand-alone mode and in grid-connected mode**.** A model for each component of the hybrid system was realised. These models have been interconnected to analyze the dynamic behavior of the complete production system. Validations were performed by simulation in Matlab/Simulink clearly demonstrated the effectiveness of the strategies proposed for the control of converters under different operation using the load demand profile and the real weather data (wind speed, solar irradiance).

Reference

1. Remus Teodorescu, and Frede Blaabjerg . Flexible Control of Small Wind Turbines With Grid Failure Detection Operating in Stand-Alone and Grid-Connected Mode, Power Electronics, IEEE Transactions on, vol . 19, no. 5, 1323 – 1332, 2004.

2. Seul-Ki Kim, Jin-Hong Jeon, Chang-Hee Cho, Jong-Bo Ahn, and Sae-Hyuk Kwon.. Dynamic Modeling and Control of a Grid-Connected Hybrid Generation System With Versatile Power Transfer. Sustainable Energy, IEEE Transactions on Industrial Electronics , Vol. 55, no. 4,July, 2008.

3. Sungwoo Bae, and Alexis Kwasinski. Dynamic Modeling and Operation Strategy for a Microgrid With Wind and Photovoltaic Resources," IEEE Transactions on smart grid. vol. 3, no. 4, pp.1867 – 1876, 2012.

4. Pablo García-Triviño , Antonio José Gil-Mena , Francisco Llorens-Iborra , Carlos Andrés García-Vázquez, Luis M. Fernández-Ramírez, Francisco JuradoPower. Control based on particle swarm optimization of grid-connected inverter for hybrid renewable energy system, Energy Conversion and Management, Vol 91 , Pages 83-92, 2015.

5. Mehdi Dali, Jamel Belhadj and Xavier Roboam. Hybrid solare-wind system with battery storage operating in grid–connected and standalone mode: Control and energy management Experimental investigation, Energy journal, 2587-2595, 2010.

6. Riad Kadri, Jean-Paul Gaubert, and Gerard Champenois. An Improved Maximum Power PointTracking for Photovoltaic Grid-Connected Inverter Based on Voltage- Oriented Control. IEEE Transations On Industrial Electronics, Vol.58, No.1: 66-75, 2011.

7. Kai Sun, Li Zhang, Yan Xing, Josep M. Guerrero. A Distributed Control Strategy Based on DC Bus Signaling for Modular Photovoltaic Generation Systems With Battery Energy Storage. IEEE Transations On Industrial Electronics, Vol.26, No.10: 66-75, 2011.

8. Nabil A. Ahmed MasafumiMiyatake, A.K. Al-Othman. Power fluctuations suppression of stand-alone hybrid generation combining solar photovoltaic/wind turbine and fuel cell systems. Energy Conversion and Management, Vol 49, No. 10:2711–2719, 2008.

9. Nahidul HoqueSamrat, Norhafizan Bin Ahmad, Imtiaz Ahmed Choudhury, and Zahari Bin Taha. Modeling, Control, and Simulation of Battery Storage Photovoltaic-Wave Energy Hybrid Renewable Power Generation Systems for Island Electrification in Malaysia. Hindawi Publishing Corporation, The Scientific World Journal, Article ID 43637, 2014.

10. Chih-Ming Hong, Ting-Chia Ou, Kai-Hung Lu. Development of intelligent MPPT (maximum power point tracking) control for a grid-connected hybrid power generation system. Energy, Vol 50, No.1: 270-279, 2013.

11. Chih-Ming Hong, Chiung-Hsing Chen. Intelligent control of a grid-connected wind photovoltaic hybrid power systems. International Journal of Electrical Power & Energy Systems , Vol 55: 554-56, 2014.

12. Mahmoud M. Amin, Osama A. Mohammed. Development of High-Performance Grid-Connected Wind Energy Conversion System for Optimum Utilization of Variable Speed Wind Turbines. IEEE Transactions On Sustainable Energy, Vol. 2, no. 3, 2011.

13. Jayalakshmi N. S, D. N. Gaonkar, Pramod Bhat Nempu. Power Control of PV/Fuel Cell/Supercapacitor Hybrid System for Stand-Alone Applications. International Journal of Renewable Energy Research, Vol.6, No.2, 2016.

14. Chih-Ming Hong , Ting-Chia Ou , Kai-Hung Lu. Development of intelligent MPPT (maximum power point tracking) control for a grid-connected hybrid power generation system Vol.50: 270-279, 2013.

15. Abderrezzak Bouharchouchel, EI Madjid Berkouk, Tarrak Ghennaml. Control and Energy Management of a Grid Connected Hybrid Energy System PV -Wind with Battery Energy Storage for Residential Applications", 8th International Conference and Exhibition on Ecological Vehicles and Renewable Energies, pp.1-11.

16. G. Malla, C.N. Bhende. Voltage control of stand-alone wind and solar energy system Internarial Journal of Electrical Power and Energy System, Vol.56, pp.361-373, 2014.

17. Bouthaina Madaci , Rachid Chenni , Erol Kurt, Kamel Eddine Hemsas. Design and control of a stand-alone hybrid power system. International Journal of Hydrogen Energy, vol. 41, pp. 12485-12496, 2016.

18. T.Bogaraj , J.Kanakaraj. A Novel Energy Management Scheme using ANFIS for Independent Microgrid. International Journal of Renewable Energy Research, Vol.6, No.3, 2016.

19. Ghada Boukettaya, Lotfi Krichen. A dynamic power management strategy of a grid connected hybrid generation system using wind, photovoltaic and Flywheel Energy Storage System in residential application Energy; 71pp.148-159, 2014.